

Half-sandwich iridium(III) and rhodium(III) complexes: Synthesis, characterization and antifouling property

Keisham S. Singh^{1,*}, Prabha Devi¹, Ramila R. Gaonkar¹, Werner Kaminsky²

¹Bio-organic Chemistry Laboratory, CSIR-National Institute of Oceanography,
Dona Paula-403004, Goa, India

²Department of Chemistry, University of Washington, Seattle, Washington-98195, USA

*for correspondence; email: keisham@nio.org or keisham.sarjit@gmail.com

Ph: +91 0832-2450392; Fax: +91-0832-2450607

Abstract:

The reaction of $[(\eta^5\text{-C}_5\text{Me}_5)\text{MCl}_2]_2$, [M = Ir (**1**) or Rh (**2**)] with thiazole ligands (L) at room temperature [L = atz; 2-acetamidothiazole (**3**) or catz; 5-chloro-2-acetamidothiazole (**4**)] afforded iridium(III) and rhodium(III) complexes of the type $[(\eta^5\text{-C}_5\text{Me}_5)\text{M}(\text{L})\text{Cl}_2]$ [M = Ir; L = atz (**5**), ctz (**6**); M = Rh, L = atz (**7**), catz (**8**)]. Compounds were characterized by FTIR, NMR (¹H & ¹³C) and mass spectroscopic data. The molecular structures of two representative compounds (**5**) and (**6**) have been determined by a single-crystal X-ray diffraction. All the synthesized compounds were obtained as neutral complexes and, the ligand is coordinated to the metal in a mono-dentate fashion. The *in vitro* antibacterial activity of the synthesized compounds against ten marine fouling bacteria showed moderate to good activity against the tested marine fouling bacteria.

Keywords: Iridium, Rhodium, 2-acetamidothiazole, Marine fouling bacteria, Antifouling, Spectroscopic data, Crystal structure.

1. Introduction

Transition metal (TM) complexes in medicinal chemistry have been rapidly developed after the clinical success of some platinum complexes, namely cisplatin, carboplatin and oxaliplatin as anticancer agents [1, 2]. It is noteworthy that organometallic complexes having pi-bonded arene or cyclopentadienyl ligands facilitated in controlling the hydrophilicity and hydrophobicity which influences cell uptake and targeting [3, 4]. Organometallic complexes of Ir(III) and Rh(III) bearing Cp* ligand possess catalytic [5-7] and biological activities [8, 9]. They have displayed remarkable anticancer [10, 11], antitumor [12] and antimicrobial properties [13]. Study on antimicrobial properties of Cp*Ir(III) and Cp*Rh(III) has been progressed rapidly. For instance, iridium(III) and rhodium(III) complexes bearing dipyriddy hydrazine ligands displayed antibacterial activities [14], while some of the Cp*Iridium(III) and Cp*Rh(III) *N*-heterocyclic carbene piano-stool complexes exhibited antimicrobial properties against several microbes displaying high activity against microbe such as *Mycobacterium smegmatis* with MICs value as low as 0.45 μ M [15]. Moreover, benzimidazole [16] and picolinic hydrazone [13] complexes of iridium(III) and rhodium(III) as well as complexes of (η^5 -C₅Me₅)Ir(III) containing biguanide ligand exhibited potent antimicrobial property [17]. Literature survey revealed that antibacterial [14, 16, 18], anticancer [8, 19, 20] and antitumor [12] activities of (η^5 -C₅Me₅)Ir(III) and (η^5 -C₅Me₅)Rh(III) complexes are well studied, however, to the best of our knowledge, their antifouling properties have not been explored.

Initially, organotin compounds, TBT (tributyltin), the well-known antifouling agents have been widely used in antifouling paints for years. [21]. Use of TBT to control fouling on submerged surfaces is now completely banned in the marine environment for concerns involving toxicity and long standing harmful effect on marine organisms [22-23]. Hence, focus was on the development of new antifouling agents and/or modification of the already existing ones that are safer and eco-friendly in the marine environment. We have studied previously the synthesis and antifouling properties of (η^6 -arene) ruthenium(II) complexes containing 2-acetamidothiazole ligands [24]. In continuation of our study on antifouling compounds, herein, we describe, the synthesis, characterization and antifouling properties of iridium(III) and rhodium(III) compounds, [MCl₂(L){(η^5 -C₅Me₅)}] (M = Ir or Rh, L = 2-acetamidothiazole or 5-chloro-2-acetamidothiazole). The aim of this study is to synthesis and characterize iridium(III) and rhodium(III) organometallic complexes and evaluate their antifouling property since the earlier studies report for the analogous (*p*-cymene)Ru(II) complexes of 2-acetamidothiazole exhibited excellent activity against several fouling bacteria [24]. Compounds were manifested as active, if there is an absence of bacterial growth (bacteriostatic) around the compound loaded-disc (measured as zone of growth inhibition in

millimeter). The synthesized compounds were characterized by spectroscopic data and the molecular structures of two representative compounds (**5**) and (**6**) have been established by single crystal X-ray diffraction.

2. Experimental

2.1. General remarks:

Solvents used were of analytical grade and used as received. IrCl₃.3H₂O and RhCl₃.3H₂O were purchased from the Arrora Matthey Ltd., India, while 2-acetamidothiazole (atz) (**3**) and 5-chloro-2-acetamidothiazole (catz) (**4**) were obtained from Sigma Aldrich India. FTIR spectra were recorded using a diffused reflection spectroscopy (DRS) on a Shimadzu-8201PC spectrophotometer with sample prepared in KBr. NMR spectra were recorded on a Bruker Avance 400 MHz spectrometer at 400 (¹H) and 100 MHz (¹³C) with SiMe₄ as internal references and coupling constants are expressed in Hertz. Mass spectra were obtained using LC-MS (Shimadzu) instrument and microanalysis was Vario micro Cube Elemental Analyser. The precursor compounds [$\{\eta^5\text{-C}_5\text{Me}_5\text{IrCl}_2\}_2$] (**1**) and [$\{\eta^5\text{-C}_5\text{Me}_5\text{RhCl}_2\}_2$] (**2**) were prepared by following the method reported in the literature [25]. The thiazole ligands, 2-acetamidothiazole (**3**) and 5-chloro-2-acetamidothiazole (**4**) were obtained from Sigma Aldrich Pvt. Ltd. and used as received.

2.2. General procedure for the preparation of [$(\eta^5\text{-C}_5\text{Me}_5)\text{M}(\text{L})\text{Cl}_2$] (where M = Ir, L = atz (**5**), catz (**6**); M = Rh, L = atz (**7**), catz (**8**)):

2.2.1. Synthesis of compounds (**5** & **6**): A round bottom flask was charged with compound (**1**) (0.05 g, 0.0627 mmol), thiazole ligand, **3** (0.0181 g, 0.127 mmol) or **4** (0.0224g g, 0.127 mmol) methanol (30 mL). The reaction mixture was stirred at room temperature. The initial red solution turned into orange colour as the reaction progressed. The reaction was stirred for 5 hrs, then the solution was rotary evaporated to 5 mL. Addition of excess diethyl ether induced yellow. The solid was collected by centrifuge and washed with diethyl ether (2 x 10 mL).

2.2.2. Synthesis of compounds **7** & **8**: The compounds was prepared following a similar method employed for **5** & **6** using the compound **2** (0.05g, 0.0808 mmol) and thiazole ligand, **3** (0.024g, 0.169 mmol) or **4** (0.0298g, 0.169 mmol) affording the compounds **7** & **8** as orange red solid.

Yield and spectroscopic data are as follows:

[IrCp*(atz)Cl₂] (**5**): Yield, 0.058 g (85%), Yellow solid, Anal. Calcd. for C₁₅H₂₁Cl₂IrN₂OS: C, 33.33; H, 3.92; N, 5.18; S, 5.93, Found: C, 33.46; H, 3.98; N, 5.27; S, 6.04. FT-IR (KBr, cm⁻¹): 3122, 3022, 1697, 1546; ¹H NMR (CDCl₃, δ): 1.54 (s, 15H, C₅Me₅), 2.30 (s, 3H, Me), 6.98 (d, 1H, J = 4), 7.71

(d, 1H, $J = 4$), 12.38 (s, 1H, NH); ^{13}C NMR (CDCl_3 , δ): 8.71, 23.18, 86.28, 112.92, 139.82, 160.91, 168.14; ESI-MS, $m/z = 505$ $[\text{M}-\text{Cl}]^+$, 405 $[\text{M}-\text{C}_5\text{Me}_5]^+$, 363 $[\text{M}-\text{Cl}-\text{atz}]^+$.

$[\text{IrCp}^*(\text{catz})\text{Cl}_2]$ (**6**): Yield, 0.065 g (90%), Yellow solid, Anal. Calcd. for $\text{C}_{15}\text{H}_{20}\text{Cl}_3\text{IrN}_2\text{OS}$: C, 31.33; H, 3.51; N, 4.87; S, 5.58, Found: C, 31.67; H, 3.63; N, 5.12; S, 5.61. FT-IR (KBr, cm^{-1}): 3115, 3010, 1697, 1543, 1521; ^1H NMR (CDCl_3 , δ): 1.56 (s, 15H, C_5Me_5), 2.29 (s, 3H, Me), 7.58 (s, 1H, Ar-H), 12.21 (s, 1H, NH), ESI-MS, $m/z = 503$ $[\text{M}-2\text{Cl}]^+$, 404 $[\text{M}-\text{C}_5\text{Me}_5-\text{Cl}]^+$, 363 $[\text{M}-\text{Cl}-\text{catz}]^+$.

$[\text{RhCp}^*(\text{atz})\text{Cl}_2]$ (**7**): Yield, 0.056 g (77%), yellow solid, Anal. Calcd. for $\text{C}_{15}\text{H}_{21}\text{Cl}_2\text{RhN}_2\text{OS}$: C, 39.93; H, 4.69; N, 6.21; S, 7.11, Found: C, 40.06; H, 4.58; N, 6.11; S, 7.06. FTIR (KBr, cm^{-1}): 3113, 2999, 1697, 1544, 1500; ^1H NMR (CDCl_3 , δ): 1.51 (s, 15H, C_5Me_5), 2.25 (s, 3H, Me), 6.94 (d, 1H, $J = 3.88$), 7.64 (d, 1H, $J = 3.92$), 12.42 (s, 1H, NH). ESI-MS, $m/z = 469$ (M-2Cl), 504 (M-Cl) $^+$.

$[\text{RhCp}^*(\text{catz})\text{Cl}_2]$ (**8**): Yield, 0.07 g (89%), yellow solid, Anal. Calcd. for $\text{C}_{15}\text{H}_{20}\text{Cl}_3\text{RhN}_2\text{OS}$: C, 37.10; H, 4.15; N, 5.77; S, 6.62, Found: C, 37.61; H, 4.11; N, 5.97; S, 6.91. (KBr, cm^{-1}): 3109, 2914, 1697, 1541; ^1H NMR (CDCl_3 , δ): 1.61 (s, 15H, Cp^*), 2.31 (s, 3H, Me), 7.55 (s, 1H), 12.51 (br 1H, NH); ESI-MS, $m/z = 415$ (M-2Cl) $^+$.

2.3. Crystal structure analysis and refinement

Crystal of compounds (**5** and **6**) suitable for X-ray analysis were grown by slow diffusion of hexane into dichloromethane solution of the complexes. The X-ray diffraction data were collected at 100 (2) K and 90 (2) K for compounds (**5**) and (**6**), respectively, on a Nonius Kappa CCD FR590 single crystal X-ray diffractometer, using $\text{MoK}\alpha$ radiation ($\lambda = 0.71073 \text{ \AA}$). The distance between crystal-to-detector was 40 mm and exposure time was 10 and 20 seconds per degree for compounds (**5**) and (**6**), respectively. Data collection were 99.9% and 99.4% completeness to 25° in θ . The data integration, cell refinement for absorption correction was performed using hkl-SCALEPACK [26]. The structures were solved by direct methods (SHELXT) [27] and refined using full matrix least squares base on F^2 (SHELXL) [28]. Refinement converged at a final R , 0.0203 and 0.0272 (for observed data F), whereas, wR_2 are 0.0483 and 0.0615 for compounds (**5**) and (**6**), respectively. Crystal structure of compounds (**5**) and (**6**) are shown in Figures 1 and 2. Data collection parameters and selected bond lengths and angles are presented in Table 1 and 2.

2.4. Bioassay for determining antifouling activity

The precursor compounds (**1** & **2**) free ligands (**3- 4**) and the synthesized compounds (**5-8**) were evaluated for their *in vitro* antibacterial activity according to Kirby-Bauer disc diffusion method [29] using the procedure as described earlier [30]. The fouling bacteria (*Aeromonas hydrophila*,

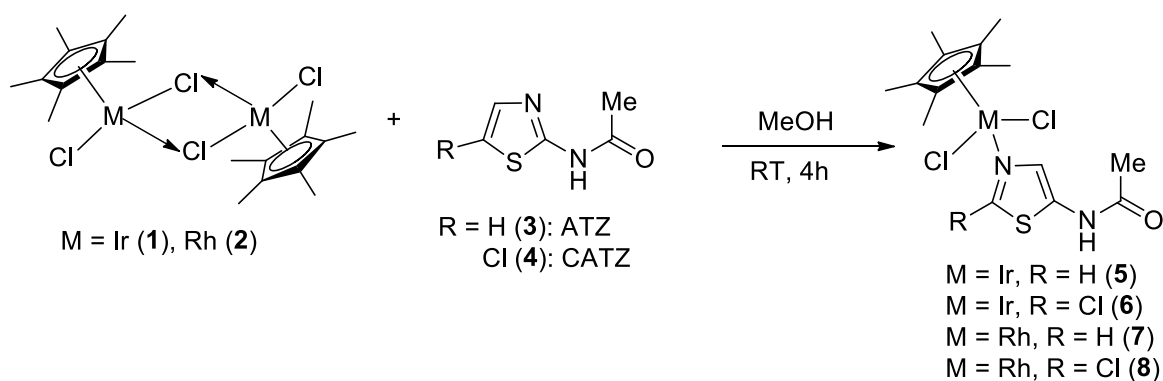
Aeromonas salmonicida, *Alcanivorax borkumensis*, *Aliivibrio salmonicida*, *Alcanivorax sp.*, *Erythrobacter litoralis*, *Planococcus donghaensis*, *Pseudomonas mendocina*, *Pseudoalteromonas sp.*, *Vibrio furnissii*) used for screening were isolated from the coastal waters of Goa and identified using standard protocol [31]. In a typical experiment, complexes (**1-8**) were dissolved in methanol/DMSO and loaded onto sterile paper discs (Whatmann No. 1 GF/C, diameter = 6 mm) at concentrations of 25 µg per disc. Discs containing solvents (methanol/DMSO) used for dissolving the compounds were used as negative control and standard antibiotic discs of streptomycin (25 µg/disc) were used as positive control. All the discs were placed aseptically on Mueller-Hinton agar plates containing a lawn of the test bacterium (spread plated with approx. 1.2×10^8 CFU/ml of test bacterium) and incubated at 35°C for 24h. The compound under study diffused into the agar and inhibited growth of the test organism to form a clear inhibition zone around the disc. After the incubation, the diameter of growth-inhibition zone formed around each of the disc was measured in millimetres using a vernier calliper. All experiments were performed in duplicate.

3. Results and discussion:

3.1. *Synthesis and characterization of iridium(III) and rhodium(III) complexes*: The reaction of $[MCl_2(\eta^5-C_5Me_5)]$ [where; M = Ir (**1**), Rh (**2**)] with 2-acetamidothiazole (atz) (**3**) or 5-chloro-2-acetamidothiazole (catz) (**4**) stirring at room temperature for 4-5 h afforded the half sandwich complexes of general formula $[MCl_2(L)(\eta^5-C_5Me_5)]$ (M = Ir, L = atz (**5**); M = Ir, L = catz (**6**); M = Rh, L = atz (**7**), M = Rh, L = catz (**8**)) (Scheme 1). The compounds were obtained as yellow (**5 & 6**) or orange red (**7 & 8**) solid in excellent yield (77-90%) and were found to be soluble in chlorinated solvents, methanol, ethanol and dimethylsulfoxide but insoluble in non-polar solvents. Compounds (**5-8**) were characterized by FT-IR, NMR and mass spectral data (see experimental section). IR spectra of the complexes showed absorption bands in the region of 2999-3122 cm^{-1} due to the N-H stretching frequency of the coordinated ligand while the C-H of aromatic ring appeared at around 1543 cm^{-1} . The complexes showed a strong peak at around 1697 cm^{-1} corresponding to the stretching frequency of $\nu_{C=O}$ of the amide group while the $\nu_{C=O}$ of the free ligands (**3**) and (**4**) showed at 1683 and 1691 cm^{-1} , respectively [32]. The $\nu_{C=O}$ of the complexes did not show shifting to lower frequency as compared to free ligand indicating C=O did not coordinated to the metal ion instead thiazole ligand is coordinated to the metal ion through N-atom only which is confirmed by spectroscopic data and crystal structure determination for compounds (**5-6**) (Figure 1 & 2). Attempts to prepare cationic chelate compounds of the type $[MCl(L)_2(\eta^5-C_5Me_5)]^+$ and $[MCl(N^{\wedge}O)(\eta^5-C_5Me_5)]^+$, respectively were not successful, Proton NMR spectrum of compound **5** displayed a signal for the methyl proton of $\eta^5-C_5Me_5$ group at 1.54 ppm whereas the methyl proton of the coordinated

2-acetamidothiazole ligand appeared at 2.30 ppm. The spectrum also showed a signal at around 12.38 ppm which is assignable to the NH group of the coordinated 2-acetamidothiazole ligand. The ^1H NMR spectrum of compound (**5**) also showed a doublet at δ 6.98 and 7.71 ppm due to aromatic proton of the coordinated thiazole ligand.

The ^{13}C -NMR spectrum of the compound (**5**) exhibited signals for methyl and ring carbon atoms of $\eta^5\text{-C}_5\text{Me}_5$ at 8.71 and 86.28 ppm, respectively, while the signal for C=O group of the 2-acetamidothiazole ligand appeared at 168.14 ppm. The proton NMR spectra of the compounds (**6-8**) showed a similar pattern except that the singlet was observed at around 7.55 ppm for compounds (**6**) and (**8**) corresponding to the aromatic proton of the thiazole ring instead of the doublet observed in the case of compounds (**5**) and (**7**). The mass spectra of compounds (**5-8**) showed peaks at m/z 469, 503, 379 and 415, corresponding to the molecular ion peak $[\text{M}-2\text{Cl}]^+$ of compounds (**5-8**), respectively. Spectroscopic data of the compounds (**5-8**) are in well agreement with their proposed structure of compounds (**5-8**).



Scheme 1. Reaction pathway for the synthesis of Compounds (**5-8**).

3.2. Crystal structure

Solid state structures of two representative compounds (**5** & **6**) have been established by single-crystal X-ray diffraction. Details of crystallography data collection for compounds (**5**) and (**6**) are given in Table 1. Selected bond lengths (\AA) and angles ($^\circ$) for **5** and **6** were presented in Table 2. Figures 1 and 2 shows ORTEP [33] diagram of compounds (**5**) and (**6**) with thermal ellipsoid at 50% probability level. Compounds (**5**) and (**6**) crystallize in a monoclinic crystal system with space groups $\text{P}2_1/c$ and $\text{C}2/c$ for **5** and **6**, respectively. Both complexes adopt a piano stool conformation where $\eta^5\text{-C}_5\text{Me}_5$ occupies three coordination sites while the remaining ones were occupied by two chloride ions and a nitrogen atom of the coordinated ligand. The average bond distance of iridium to the Cp^* ring carbons for compounds (**5**) and (**6**) are 2.1498 and 2.1512 \AA , respectively. The iridium

ion in both the structures **5** and **6** are not equidistance to the five coordinated Cp* ring carbons but slightly twisted as evident by the longer bond distance for Ir-C3 and Ir-C4 (2.164 (3) and 2.170 (4) Å) compared to the Ir-C bond distances for the remaining ring carbons of **5** which have bond distances in the range of 2.123 (4) to 2.147 (3) Å. Similarly, Ir-C3 and Ir-C4 bond distances of compound (**6**) is slightly longer than the remaining three Ir-carbon bond distances of Cp* ring carbons. The structures showed that the 2-acetamidothiazole ligand is coordinated in monodentate fashion leaving the compound neutral, which confirms the formulation of the compounds deduced by spectroscopic data. The average Ir-C bond distances in compounds (**5**) and (**6**) are 2.150 (3) and 2.151 (4) Å, respectively comparable to the reported Ir-C bond distances for the [Cp*Ir(tpn)Cl] (tpn = tropolonato) [34]. The C-C bond distances of the cyclopentadienyl ring in both the complexes are comparable indicating delocalization of pi-electron in the ring.

Further, Ir-Cl(1) and Ir-Cl(2) bond lengths for compound **5** is equal to 2.437 (7) Å however, for compound **6**, Ir-Cl (2) (2.4213(11) Å) bond distance is slightly longer than Ir-Cl(1) (2.4100 (10) Å), but the values of Ir-Cl in both the compounds **5** & **6** are within the range of reported Ir-Cl bond lengths found in other Cp*Ir(III) complexes such as Cp*Ir(III)naphthylpyridine (2.4123 (3) Å) [35], Cp*Ir(III) bearing 1,2,3-benzothiadiazole (2.4097 (6) Å) [36] and Cp*Ir(III)NHC complex with imidazolin-2-ylidene ligand (2.4213 (19) Å) [37]. The Ir-N bond distances for compounds (**5**) and (**6**) are 2.126 (2) and 2.136 (3) Å, respectively, and values are comparable to those reported for Cp*Ir(III) 1,2,3-benzothiadiazole complex (2.119(2) Å) [36] where ligand is coordinated to iridium in unchelated fashion. However, the Ir-N bond distance is slightly longer than those reported for Cp*Ir(III) complex containing 2-(pyridine-2-yl)thiazole *N,N*-chelating ligand (2.070 (10) Å) [38] suggesting that Ir-N bond distance for chelated ligands are slightly shorter than the non-chelated ligand. The Cl(1)-Ir-Cl(2), Cl(1)-Ir-N(1) and Cl(2)-Ir-N(2) bond angles for both the compounds **5** and **6** (Table 2) are close to other related Cp*Ir(III) imidazole complex [36].

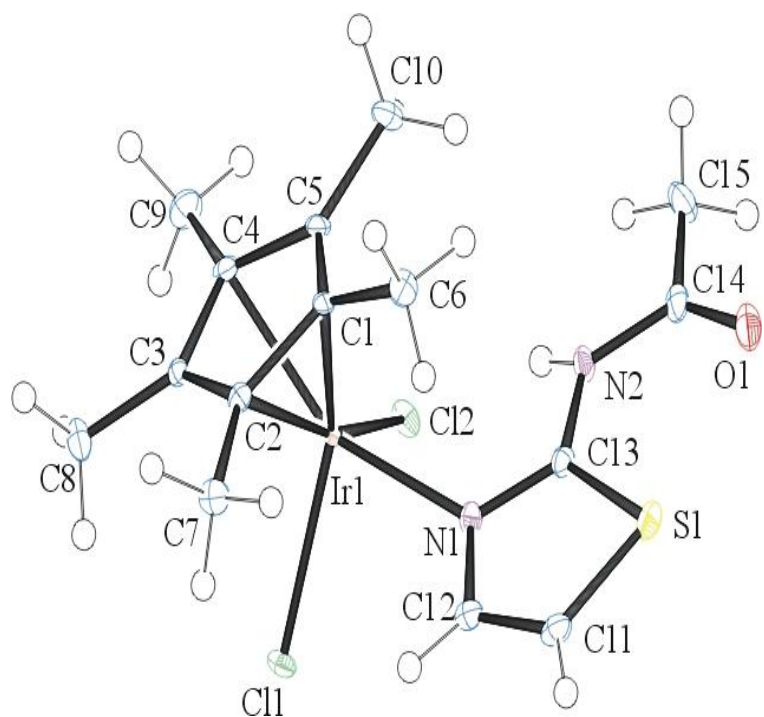


Figure 1. ORTEP diagram of compound **(5)**. Thermal ellipsoids are drawn at the 50% probability level.

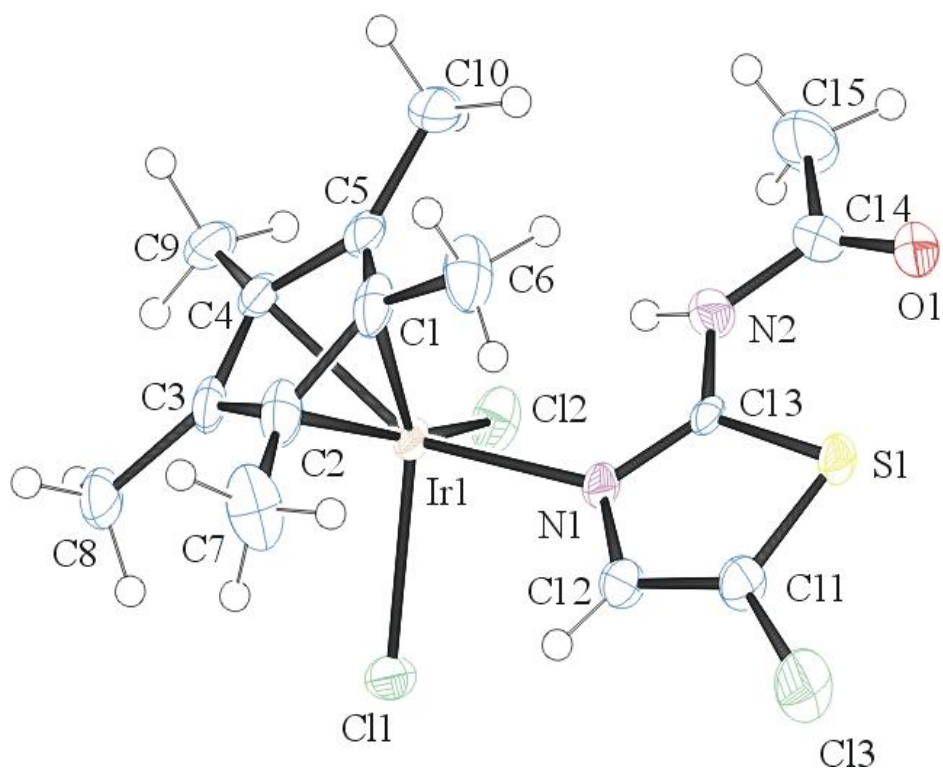


Figure 2. ORTEP diagram of compound **(6)**. Thermal ellipsoids are drawn at the 50% probability level.

3.3. Biological assay

Antibacterial properties of the synthesized compounds (**5-8**) was evaluated against 10 marine fouling bacteria (Table 3). In general, the compounds exhibited mild to good activity against test bacteria as revealed from the growth inhibition zones around the discs (Figure 3 & 4). Figures 3 and 4 showed the antibacterial activity against the fouling bacteria for Iridium (**5 & 6**) and rhodium (**7 & 8**) compounds as compared to free ligands (**3 & 4**) and precursor compounds, $[(Cp^*MCl_2)_2]$ (M = Ir (**1**); Rh (**2**)), respectively. As evident from Figure 3 and 4 the precursor complexes 1 and 2 as well as free ligands 3 & 4 displayed insignificance activity as compared to the compounds (5-8) and standard streptomycin against the tested fouling bacteria. The precursor compound (**1**) exhibited a weak activity only against *Aeromonas hydrophila*, *Alcanivorax borkumensis* and *Aliivibrio salmonicida* among the ten tested bacteria (Figure 3). Similarly, the precursor compound (**2**) and the ligand did not show significance activity against the tested bacteria except a weak activity observed against *Erythrobacter litoralis* and *Pseudoalteromonas sp.* (Fig 4). As compared to iridium compounds (**5 & 6**), rhodium compounds (**7 & 8**) exhibited a mild activity and were sensitive to the growth of six and four bacterial cultures, respectively. On the other hand iridium compounds (**5 & 6**) showed better activity than the rhodium compounds (**7 & 8**) with seven bacterial cultures being sensitive to compound (**5**) and eight to compound (**6**). Compound (**6**) which contained a chloride substituent in the thiazole ring exhibited significantly higher activity than compound (**5**). Figure 5 showed growth inhibition zone for compound (**6**) against fouling bacteria, *Aeromonas hydrophila* and *Pseudoalteromonas sp.* It displayed activity against eight of the ten tested bacterial cultures showing growth inhibition zone between 2-9 mm. Interestingly, fouling bacteria *Aeromonas salmonicida*, *Alcanivorax borkumensis* and *Aliivibrio salmonicida* which were not sensitive to standard streptomycin were found to be sensitive to one or more of these complexes. For example, *Aeromonas salmonicida* was sensitive to compounds (**5-7**), while *Alcanivorax borkumensis* was sensitive to compounds (**6**) and (**7**) and *Aliivibrio salmonicida* was sensitive to compound (**5**).

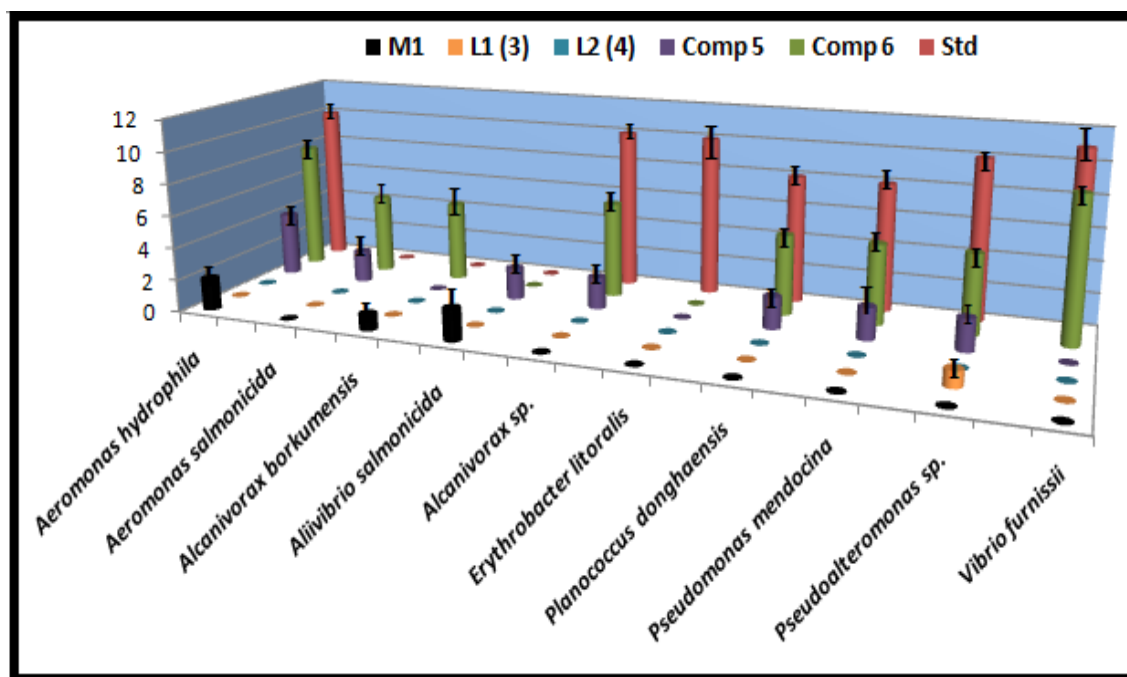


Figure 3. Antifouling activity of precursor Iridium compound (1), free ligands (3 & 4), iridium acetamidothiazole compounds (5 & 6) and standard streptomycin against ten marine fouling bacteria [(M1= compound (1); L1= compound (3), L2 = compound (4)].

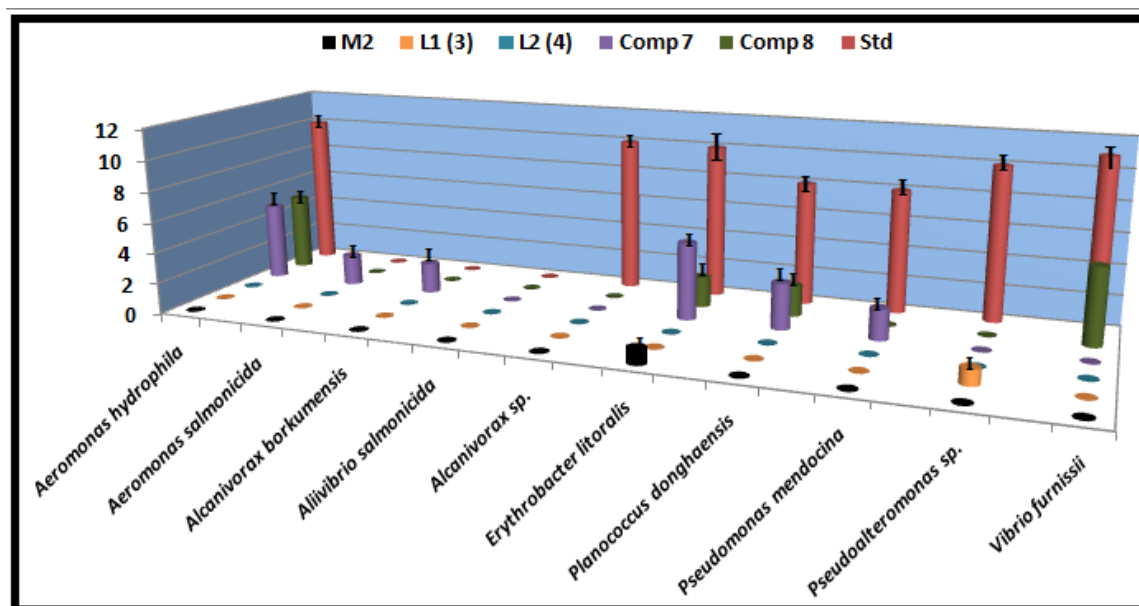


Figure 4. Antifouling activity of precursor rhodium compound (2), free ligands (3 & 4) and rhodium acetamidothiazole compounds (7 & 8) and standard streptomycin against ten marine fouling bacteria.

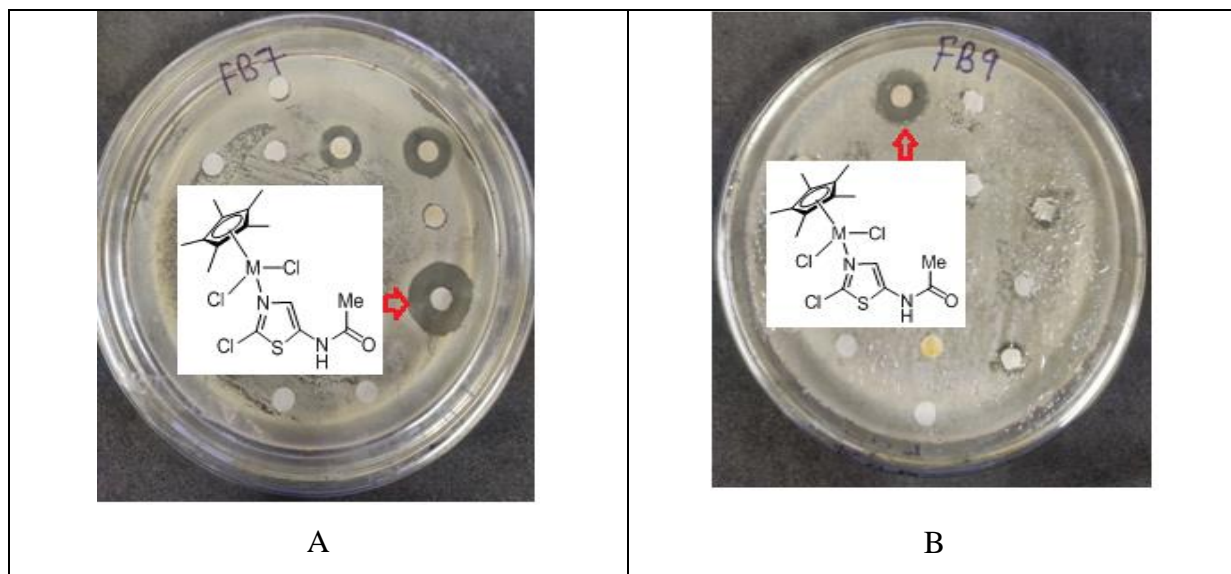


Figure 5. Disc showing inhibition zone for compound (**6**) against *Alcanivorax borkumensis* (A) and *Pseudoalteromonas sp.* (B).

Transition metal complexes have great potential as metal-based antibacterial [39], anticancer and therapeutic agents [40-42]. Specifically, ruthenium, iridium and rhodium have been attracted in the study of transition metal complexes with therapeutic potential [43-46]. Lu and co-workers [47] as well as Kollipara and his group [13, 48] tested antimicrobial activities of a series of rhodium(III) and Iridium(III) complexes. They showed that several of their complexes possessed activity against clinical pathogens and a few of the complexes have shown better activity than the standard gentamycin/ciprofloxacin. Very recently, Hohlfeld et al. described antimicrobial property of Cp* Ir(III) dipyrinato complex that showed inhibition against the Gram positive bacteria [49]. Antibacterial activity of transition metal complexes is influenced by the coordinating ligand. Usually, the presence of N or S donor ligand in the complexes contribute to antibacterial activity of metal complexes. Previously, it was reported that a thiazole ring in a compound dramatically increased antibacterial [50] and antiviral [51] activities, likely due to the presence of a –N=C-S group in the thiazole moiety [52]. Therefore, we believed that the activity of our synthesized compounds (**5-8**) could be due to the presence of 2-acetamidothiazole ligand. Further, compound (**6**) showed better activity than **5** indicating that biological activity is enhanced in the presence of an electron withdrawing group within the thiazole ring.

Table 1: Summary of Crystal structure determination and refinement parameters for compounds **5** and **6**

Empirical formula	C ₁₅ H ₂₁ Cl ₂ IrN ₂ OS Compound (5)	C ₁₅ H ₂₀ Cl ₃ IrN ₂ OS Compound (6)
CCDC	2184576	2184575
Formula weight	540.50	574.94
Temperature	100(2) K	90(2) K
Wavelength	0.71073 Å	0.71073 Å
Crystal system	Monoclinic	Monoclinic
Space group	P 21/c	C 2/c
Unit cell dimensions		
a (Å)	8.0090 (10)	18.7689(2)
b (Å)	12.6451(2)	16.7760(2)
c (Å)	17.2082(3)	13.6663(2)
α (°)	90	90
β (°)	90.1930(10)	117.9900(10)
γ (°)	90	90
Volume	1742.74(5)	3799.74(9) Å ³
Z	4	8
Density (calculated)	2.060 Mg/m ³	2.010 Mg/m ³
Absorption coefficient	8.090 mm ⁻¹	7.563 mm ⁻¹
F(000)	1040	2208

Crystal size	0.300 x 0.280 x 0.260 mm ³	0.210 x 0.100 x 0.100 mm ³
θ range for data collection (°)	1.999 to 28.279	1.727 to 28.294
Index ranges	$-10 \leq h \leq 10$ $-16 \leq k \leq 16$ $-22 \leq \ell \leq 22$	$-24 \leq h \leq 24$ $-22 \leq k \leq 22$ $-18 \leq \ell \leq 18$
Reflections collected	8405	9071
Independent reflections [R_{int}]	4311 [0.0330]	4662 [0.0341]
Completeness to theta = 25.000°	99.9 %	99.4 %
Final R indices [$I > 2\sigma(I)$]	$R_1 = 0.0203$, $wR_2 = 0.0483$	$R_1 = 0.0272$, $wR_2 = 0.0615$
R indices (all data)	$R_1 = 0.0231$, $wR_2 = 0.0491$	$R_1 = 0.0334$, $wR_2 = 0.0635$
Largest different peak and hole	1.252 and -1.155 e.Å ⁻³	2.548 and -1.241 e.Å ⁻³

Table 2. Selected bond lengths (Å) and angles (°) for compounds (5) and (6) with estimated standard deviation in parenthesis.

<i>Bond lengths</i>	Compound (5)	Compound (6)	<i>Bond lengths</i>	Compound (5)	Compound (6)
Ir(1)-C(1)	2.145 (3)	2.136 (4)	Ir(1)-N(1)	2.126 (2)	2.136 (3)
Ir(1)-C(2)	2.123 (3)	2.130 (4)	Ir(1)-Cl(1)	2.437 (7)	2.4100 (10)
Ir(1)-C(3)	2.164 (3)	2.165 (4)	Ir(1)-Cl(2)	2.437 (7)	2.4213 (11)
Ir(1)-C(4)	2.170 (3)	2.169 (4)	N(1)-C(13)	1.327 (4)	1.318 (5)
Ir(1)-C(5)	2.147 (3)	2.156 (4)	C(14)-O(1)	1.223 (4)	1.221 (5)
C(13)-S(1)	1.722 (3)	1.712 (4)	N(2)-C(14)	1.360 (4)	1.366 (5)
<i>Bond angles</i>					
Cl(1)-Ir(1)-Cl(2)	90.17 (2)	89.88 (9)	C(13)-N(2)-C(14)	124.6 (3)	123.2 (4)
N(1)-Ir(1)-Cl(1)	85.77 (7)	85.03 (8)	N(2)-C(14)-O(1)	121.7 (3)	121.5 (4)
N(1)-Ir(1)-Cl(2)	90.35 (7)	89.88 (9)	N(2)-C(14)-C(15)	114.8 (3)	114.0 (4)

Table 3. Results of antifouling screening for compounds (1-8) showing zones of inhibition values (in mm) against fouling bacteria.

S. No.	<i>Aeromonas hydrophila</i> FB3	<i>Aeromonas salmonicida</i> FB4	<i>Alcanivorax bor-kumensis</i> FB7	<i>Aliivibrio salmonicida</i> FB8	<i>Alcanivorax</i> sp. FB1	<i>Erythrobacter litoralis</i> FB5	<i>Planococcus donghaensis</i> FB2	<i>Pseudomonas mendocina</i> FB6	<i>Pseudoalteromonas</i> sp. FB9	<i>Vibrio furnissii</i> FB10
Compd. (1)	1.8±0.2	0	1±0	1.2±0.2	0	0	0	0	0	0
Compd. (2)	0	0	0	0	0	0.8±0.2	0	0	0	0
Compd. (3)	0	0	0	0	0	0	0	0	1±0	0
Compd. (4)	0	0	0	0	0	0	0	0	0	0
Compd. (5)	4.1±0.1	1.9±0.1	0	1.9±0.1	1.9±0.1	0	2±0.2	1.6±0.5	2±0.1	0
Compd. (6)	8.1±0.1	5±0.2	4.7±0.6	0	6.1±0.1	0	5±0.2	5±0.1	5±0.2	8.8±0.2
Compd. (7)	5±0.1	2±0.1	2±0.1	0	0±0.1	5±0.1	3±0.2	2±0.1	0	0
Compd. (8)	5±0.1	0	0	0	0	2±0.1	2±0.1	0	0	4.9±0.1
Strep	10±0.1	0	0	0	10±0.1	10.5±0.5	7.9±0.2	7.9±0.3	9.8±0.3	10.7±0.6

The activity data for the compounds 1-8 and standard (streptomycin) are expressed as a measured of the inhibition zones (mm) at concentration 25µg/disc. The values given in the data are the mean of two replicates.

Conclusion

We described the synthesis, spectral characterization, X-ray structure, and antifouling evaluation of four neutral half sandwich iridium(III) and rhodium(III) complexes containing 2-acetamidodiazole ligands. Iridium compound (6) with chloride substituted in thiazole ring exhibited higher antifouling activity being sensitive to eight of the ten tested fouling bacteria when compared to the analogous non-chlorinated thiazole ligand coordinated iridium compound (5). Three of the fouling bacteria were not affected by the standard streptomycin but they appeared to be sensitive to several of these compounds (5-8). This result indicates that iridium(III) and rhodium(III) compounds have potential as antibacterial agents against fouling bacteria. The ligand coordinated to the complexes tune the biological activity as evident from much lower activity or being non-active shown by their free metal precursor compounds (1 & 2). Further, exploring on the synthesis of antifouling agents based on

metal complexes specifically with less expensive metal such as zinc and iron is desirable for the development of economically viable and environmental friendly antifouling agents to replace toxic tributyltin (TBT) compounds.

Supplementary material

CCDC Nos. 2184575 and 2184576 contain the supplementary crystallography data for this article. These data can be obtained free of charge via <http://www.ccdc.cam.ac.uk/conts/retrieving.html> or from the Cambridge Crystallography Data Center, 12 Union Road, Cambridge CB21 E2, UK. Fax: (+44) 1223 336 033; E-mail: deposit@ccdc.cam.ac.uk.

Acknowledgements

We thank CSIR, India for financial support through Bioprosmar project (MLP2019). We sincerely thank the anonymous reviewers for their helpful suggestions. KSS and PD are grateful to the Director, CSIR-NIO for his constant encouragement and Prof. Sunder Dhuri, School of Chemical Sciences, Goa University for providing elemental analysis data.

References

- [1] L. Kelland, *Nat. Rev. Cancer*, **7**, 573 (2007).
- [2] D. Wang, S. J. Lippard, *Nat. Rev. Drug. Discov.*, **4**, 307 (2005).
- [3] M. G. Mendoza-Ferri, C. G. Hartinger, M. A. Mendoza, M. Groessl, A. E. Egger, R. E. Eichinger, J. B. Mangrum, N. P. Farrell, M. Maruszak, P. J. Bednarski, F. Klein, M. A. Jakupec, A. A. Nazarov, K. Severin, B. K. Keppler, *J. Med. Chem.*, **52**, 916 (2009).
- [4] R. E. Aird, J. Cummings, A. A. Ritchie, M. Muir, R. E. Morris, H. Chen, P. J. Sadler, D. I. Jodrell, *Br. J. Cancer*, **86**, 1652 (2002).
- [5] S. Mochida, N. Umeda, K. Hirano, T. Satoh, M. Miura, *Chem. Lett.*, **39**, 744 (2010).
- [6] K. Shin, Y. Park, Mu-Hyun Baik, S. Chang, *Nature Chem.*, **10**, 218 (2018).
- [7] G. Song, F. Wang, X. Li, *Chem. Soc. Rev.*, **41**, 3651 (2012).
- [8] Z. Liu, P. J. Sadler, *Acc. Chem. Res.*, **47**, 1174 (2014).
- [9] C. H. Leung, H. J. Zhong, D. S. H. Chan, D. L. Ma, *Coord. Chem. Rev.*, **257**, 1764 (2013).
- [10] Y. Geldmacher, M. Oleszak, W. S. Sheldrick, *Inorg. Chim. Acta*, **393**, 84 (2012).
- [11] O. Dömötör, S. Aicher, M. Schmidlehner, M. S. Novak, A. Roller, M. A. Jakupec, W. Kandioller, C. G. Hartinger, B. K. Keppler, É. A. Enyedy, *J. Inorg. Biochem.*, **134**, 57 (2014).
- [12] G. S. Yellol, A. Donaire, J. G. Yellol, V. Vasylyeva, C. Janiak, J. Ruiz, *Chem. Commun.*, **49**, 11533 (2013).

- [13] N. R. Palepu, J. R. Premkumar, A. K. Verma, K. Bhattacharjee, S.R. Joshi, S. Forbes, Y. Mozharivskyj, K. M. Rao, *Arabian J. Chem.*, **11**, 714 (2015).
- [14] B. P. R. Aradhyula, N. Joshi, K. M. Poluri, M. R. Kollipara, *J. Mol. Struct.*, **1164**, 191 (2018).
- [15] C. M. Bernier, C. M. DuChane, J. S. Martinez, J. O. Falkinham III, J. S. Merola, *Organometallics*, **40**, 1670 (2021).
- [16] N. Baartzes, A. Jordaan, D. F. Warner, J. Combrinck, D. Taylor, K. Chibale, G. S. Smith, *Eur. J. Med. Chem.*, **206**, 112694 (2020).
- [17] F. Chen, J. Moat, D. McFeely, G. Clarkson, I. J. Hands-Portman, J. P. Furner-Pardoe, F. Harrison, C. G. Dowson, P. J. Sadler, *J. Med. Chem.*, **61**, 7330 (2018).
- [18] A. Lapasam, V. Banothu, U. Addepally, M. R. Kollipara, *J. Chem. Sci.* **132**, 34 (2020).
- [19] K. Málíková, L. Masaryk, P. Štarha, *Inorganics*, **9**, 26 (2021).
- [20] J. J. Li, L. Guo, Z. Tian, M. Tian, S. Zhang, K. Xu, Y. Qian, Z. Liu, *Dalton Trans.*, **46**, 15520 (2017).
- [21] E. D. Goldberg, *Environment*, **28**, 17 (1986).
- [22] G. W. Bryan, P.E. Gibbs, in: M.C. Newman, A.W. McIntosh, (Eds), *Metal Ectotoxicology: Concepts and Applications*, Lewis Publishers Inc., Boston, **323** (1991).
- [23] C. Alzieu, *Ecotoxicology*, **9**, 71 (2000).
- [24] K. S. Singh, P. Devi, S. G. Sawant, W. Kaminsky, *Polyhedron*, **100**, 321 (2015).
- [25] R.G. Ball, W.A.G. Graham, D. M. Heinekey, J.K. Hoyano, A.D. McMaster, B.M. Mattson, S.T. Michel. *Inorg. Chem.* **29**, 2023 (1990).
- [26] Z. Otwinowski, W. Minor, In: *Methods in Enzymology*, C. W. Carter, Jr. R. M. Sweet (Eds.) Academic Press: New York, **276**, 307 (1997).
- [27] Sheldrick G. M. SHELXT - Integrated space-group and crystal-structure determination. *Acta Cryst.*, **A71**, 3 (2015).
- [28] G.M. Sheldrick. Crystal structure refinement with SHELXL. *Acta Cryst.*, **C71**, 3 (2015).
- [29] A.W. Bauer, W.M.M. Kirby, J.C. Sherris, M. Turck, *Am. J. Clin. Pathol.*, **45**, 493 (1966).
- [30] P. Devi, S. Wahidullah, C. Rodrigues, L. D'Souza, *Mar. Drugs*, **8**, 1203 (2010).
- [31] H.M. Dalton, L.K. Poulsen, P. Halasz, M.L. Angles, A.E. Goodman, K.C. Marshall, *J. Bacteriol.*, **176**, 6900 (1994).
- [32] M. N. Hughes and K. J. Rutt, *J. Chem. Soc. Dalton Trans.*, 1311 (1972).
- [33] L. Farrugia, *J. Appl. Cryst.*, **30**, 565 (1997).

- [34] K. S. Singh, W. Kaminsky, *J. Coord. Chem.*, **67**, 3252 (2014).
- [35] K. T. Prasad, B. Therrien, K. M. Rao, *J. Organomet. Chem.*, **693**, 3049 (2008).
- [36] D. A. Bashirov, T. S. Sukhikh, N. V. Kuratieva, D. Y. Naumov, S. N. Konchenko, N. A. Semenov, A. V. Zibarev, *Polyhedron*, **42**, 168 (2012).
- [37] R. Corberán, M. Sanau, E. Peris, *Organometallics*, **26**, 3492 (2007).
- [38] M. Gras, B. Therrien, G. Süß-Fink, A. Casini, F. Edeffe, P. J. Dyson, *J. Organomet. Chem.*, **695**, 1119 (2010).
- [39] S. N. Sovari, F. Zobi, *Chemistry*, **2**, 418 (2020).
- [40] Z. Guo, P. J. Sadler, *Angew. Chem. Int. Ed.*, **38**, 1512 (1999).
- [41] N. J. Farrer, L. Salassa, P. J. Sadler, *Dalton Trans.*, 10690 (2009)
- [42] W. H. Ang, P. J. Dyson, *Eur. J. Inorg. Chem.*, 4003 (2006).
- [43] W. H. Ang, E. Daldini, C. Scolaro, R. Scopelliti, L. Juillerat-Jeannerat, P. J. Dyson, *Inorg. Chem.*, **45**, 9006 (2006).
- [44] U. Śliwińska, F. P. Pruchnik, S. Ułaszewski, M. Latocha, D. Nawrocka-Musiał, *Polyhedron*, **29**, 1653 (2010).
- [45] O. Dömötör, S. Aicher, M. Schmidlehner, M. S. Novak, A. Roller, M. A. Jakupec, W. Kandioller, C. G. Hartinger, B. K. Keppler, É. A. Enyedy, *J. Inorg. Biochem.*, **134**, 57 (2014).
- [46] Z. Liu, A. Habtemariam, A. M. Pizarro, S. A. Fletcher, A. Kisova, O. Vrana, L. Salassa, P. C. A. Bruijninx, G. J. Clarkson, V. Brabec, P. J. Sadler, *J. Med. Chem.*, **54**, 3011 (2011).
- [47] L. Lu, L. J. Liu, W. C. Chao, H. J. Zhong, M. Wang, X. P. Chen, J. J. Lu, R. N. Li, D. L. Ma, C. H. Leung, *Sci. Rep.*, **5**, e14544 (2015).
- [48] A. Lapasam, V. Banothu, A. Uma, M. R. Kollipara, *J. Mol. Struct.*, **1191**, 314 (2019).
- [49] B. F. Hohlfeld, B. Gitter, C. J. Kingsbury, K. J. Flanagan, D. Steen, G. D. Wieland, N. Kulak, M. O. Senge, A. Wiehe, *Chem. Eur. J.*, **27**, 6440 (2021).
- [50] B. S. Holla, K. V. Malini, V. S. Rao, B. K. Sarojini, and N. S. Kumari, *Eur. J. Med. Chem.*, **38**, 313 (2003).
- [51] O. I. El-Sabbagh, M. M. Baraka, S. M. Ibrahim, C. Pannecouque, G. Andrei, R. Snoeck, J. Balzarini, A. A. Rashid, *Eur. J. Med. Chem.*, **44**, 3746 (2009).
- [52] E. Yousif, Y. Farina, K. Kasar, A. Graisa, K. Ayid, *Am. J. Appl. Sci.*, **6**, 582 (2009).